Decreasing frequency and extent of frost damage in European oaks over 1961-2021

Jianhong Lin, Nicolas Delpierre, Fabien Caroulle, Sebastien Cecchini, Vincent Badeau, Thomas Caignard, Daniel Berveiller, Sylvain Delzon, Heikki Hänninen, Antoine Kremer, et al.

Agricultural and Forest Meteorology 376 (2026) 110927

Contents lists available at ScienceDirect

Agricultural and Forest Meteorology

journal homepage: www.elsevier.com/locate/agrformet

Decreasing frequency and extent of frost damage in European oaks over 1961-2021

Jianhong Lin [a,*], Nicolas Delpierre [a,b,*], Fabien Caroulle [c], Sebastien Cecchini [d], Vincent Badeau [e], Thomas Caignard [f], Daniel Berveiller [a], Sylvain Delzon [f], Heikki Hänninen [g,h], Antoine Kremer [f], Annette Menzel [i], Alexandre Morfin [a], Julien Parmentier [f], Gaëlle Vincent [a], Rui Zhang [g,h], Cyrille Rathgeber [j]

[a] Université Paris-Saclay, CNRS, AgroParisTech, Ecologie Société Evolution, 91190 Gif-sur-Yvette, France
[b] Institut Universitaire de France (IUF), France
[c] Ministère de l'Agriculture et de la Souveraineté alimentaire, département de la santé des forêts, Paris, France
[d] Office National des Forêts, Département Recherche Développement et Innovation, 77300 Fontainebleau, France
[e] Univ Lorraine, AgroParisTech, INRAE, UMR 1434, SILVA, F-54000 Nancy, France
[f] UMR BIOGECO, INRAE, Université de Bordeaux, Cestas, France
[g] State Key Laboratory of Subtropical Silviculture, Zhejiang A&F University, Hangzhou, China
[h] SFGA Research Center for Torreya grandis, Zhejiang A&F University, Hangzhou, China
[i] Technical University of Munich, TUM School of Life Sciences, Ecoclimatology, Freising, Germany
[j] INRAE, SILVA, Université de Lorraine, AgroParisTech, Nancy, France

ARTICLE INFO

Keywords:
Late spring frost
Damage frequency
Damage extent
Leaf phenology
European oaks
Model

ABSTRACT

Late spring frosts (LSF) have substantial ecological and economic impacts in the temperate and boreal zones. Yet, the effects of climate warming on the frequency (i.e., probability of LSF in a given year, in %) and extent (i.e., percentage of trees in a population damaged by a given LSF event) of LSF damage remain underexplored. Here, extending a budburst model that accounts for within-population variability, we developed and evaluated a new model of LSF damage occurrence and extent using 1,220 observations of LSF damage to newly emerged leaves from 304 oak populations in France (1997–2021). Our model simulations reveal that overall, French oak populations are, over time, less exposed to LSF amid ongoing climate change. We observed an overall decline in the frequency (-0.22 % per year) and extent (-0.34 % per year) of LSF damage in French oak populations over the past six decades (1961–2021). These trends are largely driven by the temporal advance of both the last spring frost day and budburst dates, with the last spring frost day advancing at a slightly faster rate (-0.28 days per year) than budburst (-0.21 days per year). This temporal mismatch explains why, contrary to the common assumption that earlier budburst increases frost risk, earlier budburst was in fact associated with a lower frequency of LSF damage. Nevertheless, considerable geographical variability emerged, with declines in damage frequency being more pronounced in continental regions, whereas declines in damage extent were more pronounced in coastal regions. Our findings underscore the importance of considering both LSF frequency and extent when assessing frost risks in a warming climate, offering a comprehensive framework for future ecological and economic evaluations of LSF impacts.

1. Introduction

Late spring frost (LSF), which we define here as a frost event occurring after budburst, can cause substantial ecological damage (Hufkens *et al.* 2012; Vitasse *et al.* 2018; Vitasse *et al.* 2019) as well as economic losses (Lamichhane 2021) to forest trees, vineyards, and orchards in temperate and boreal zones. Indeed, late frost can destroy the new leaves or flowers that have just emerged after budburst, resulting in a delayed leaf phase and/or the destruction of fruit production. Several LSF events have occurred in Europe over the past few years, leading to severe economic losses. For instance, in spring 2017, LSF events occurring over 8 days (from 17 to 24 April) resulted in losses

* Corresponding authors at: Université Paris-Saclay, CNRS, AgroParisTech, Ecologie Société Evolution, 91190 Gif-sur-Yvette, France.
E-mail addresses: jianhong.lin@universite-paris-saclay.fr (J. Lin), nicolas.delpierre@universite-paris-saclay.fr (N. Delpierre).

https://doi.org/10.1016/j.agrformet.2025.110927
Received 7 March 2025; Received in revised form 4 November 2025; Accepted 5 November 2025
Available online 15 November 2025

worth €3.3 billion in Europe (Faust & Herbold 2018). Four years later, another serious LSF occurred over 3 days (from 6 to 8 April), damaging productivity and an economic loss estimated at €2 billion (Lamichhane 2021). With accelerating climate warming, the exposure of new leaves or flowers to LSF has changed over time and is likely to continue changing, thus influencing tree physiology and growth (Vitasse *et al.* 2019) with a possible impact on the productivity of forests (Gu *et al.* 2008) and even on the distribution (Chuine 2010) of tree species.

Nevertheless, current knowledge on the frequency (i.e., probability of LSF in a given year, in %) and extent (i.e., percentage of trees in a population damaged by a given LSF event) of frost damage to forest trees and their relation to ongoing climate change is very limited. To date, studies aiming to quantify changes in the frequency of frost damage have been based on indirect evidence. These studies cross-referenced temperature data (date of occurrence of sub-zero temperatures) with budburst dates (Liu *et al.* 2018; Vitasse *et al.* 2018; Ma *et al.* 2019) or tree-ring widths (Dittmar *et al.* 2006; Vitasse *et al.* 2019; Sangüesa-Barreda *et al.* 2021) to determine the occurrence of LSF episodes, highlighting different multi-decadal trends of LSF occurrence depending on the geographical location. However, this evidence is indirect because ring width is influenced by numerous factors, not only LSF, and the concurrence of budburst and sub-zero temperatures does not necessarily result in frost damage since emerging leaves have a frost resistance threshold ranging from -2 to -8°C depending on the species and leaf maturation stage (Taschler *et al.* 2004; Lenz *et al.* 2013; Vitasse *et al.* 2014; Zohner *et al.* 2020). A proper evaluation of the frequency of frost damage on leaves would require actual observations of canopies damaged by frost, which have rarely been published except at specific sites and for limited periods (typically 1 year) (Hufkens *et al.* 2012; Menzel *et al.* 2015).

Another blind spot in research is the extent of frost damage in tree populations. Previous studies have indicated that individual oak trees require up to 43 days to refoliate after frost damage, with the second flush of leaves compensating for only 25 % of the productivity lost due to a shortened growing season (Zohner *et al.* 2019) and that beech trees required 54 days to reach full maturity of the canopy again after a late spring frost damage (Menzel et al., 2015). This highlights the importance of quantifying the extent of frost damage within a population. Indeed, widespread frost damage across a forest, as opposed to isolated damages affecting only a few trees, can result in significantly greater productivity losses at the population level.

While many studies use the minimum daily temperatures between budburst and mid-July to quantify the so-called severity of LSF damage in the population (Hänninen 1991, 2016; Ma *et al.* 2019), this metric fails to quantify the proportion of trees damaged by LSF within the population. It should be noted that previous studies which quantify the "severity" of LSF damage treated the population as a homogeneous group (Hänninen 1991, 2016; Ma *et al.* 2019), neglecting the considerable individual variability of exposure to frost related to the variability of budburst within the population. Indeed, there is a considerable range in the timing of budburst within tree populations (typically ~3 weeks from the earliest to the latest trees (Delpierre *et al.* 2017; Denéchère et al. 2021)), resulting in trees at different stages of budburst coexisting during this period in the population. Compared to closed buds or mature leaves, newly emerged leaves require time to develop frost resistance, typically 1–3 weeks, depending on species and environmental conditions (Lenz *et al.* 2013). They are thus more vulnerable during this period. Considering the within-population variability of budburst and the existence of a "vulnerability window" for the new leaves, the leaves of individuals with early budburst may be exposed to frost, while others with late budburst may avoid it. Thus, in addition to assessing LSF damage at the population level, evaluating the variability in the extent of LSF damage within populations is essential.

Here, we quantify for the first time the multi-decadal trend of both the frequency and extent of frost damage in forest tree populations. For this purpose, we introduce an unprecedented dataset comprised of 1220 observations of frost damage with their occurrence and extent in France for the period 1997-2021 in 304 populations of temperate deciduous oaks (*Quercus petraea* (Matt.) Liebl. and *Quercus robur* L.), which are two of the main European forest tree species (Vitasse *et al.* 2019; Rubio-Cuadrado *et al.* 2021), representing 10 % of the European wood growing stock (24 % for France). We hypothesized that (a) multi-decadal trends in LSF occurrence vary geographically, with higher elevations and latitudes experiencing greater frost risk, and (b) LSF damage frequency and extent exhibit distinct temporal trajectories within tree populations. Specifically, we used these data to calibrate and evaluate a new process-based model to simulate the occurrence and extent of frost damage in tree populations. Using this model, we simulated the trends of the frequency and extent of LSF damage over the past six decades (1961-2021) in 304 oak populations across France. Our objectives were to evaluate (a) the changes in the frequency and extent of LSF damage across different geographic locations due to climate warming and (b) whether these temporal trends in LSF damage frequency and extent were consistent.

2. Material and methods

2.1. Observations of late spring frost damage and temperature data

The records of LSF damage in the crowns of *Quercus petraea* and *Quercus robur* trees were compiled from two complementary sources, yielding a total of 1220 site-years across 304 sites in France (Supplementary Table 1; spatial distribution in Fig. 1). In the following, we considered both species jointly (as "oaks") because they are very close phylogenetically, frequently hybridize and burst buds simultaneously in a given forest (Bacilieri *et al.* 1995; Lebourgeois *et al.* 2008). The dataset documents both the occurrence of LSF damage (i.e., whether frost damage was observed) and, for a subset of site-years, the extent of damage (i.e., the proportion of trees affected in a given event).

The first source of data consisted of 15 phenological monitoring sites, providing 67 site-years of observations (ranging from 1 to 16 years per site, average of 4 years). Among these, 13 were mature forests (11 from the RENECOFOR network, http://www1.onf.fr/renecofor/@@index.html) and two were planted common gardens of younger trees (6–15 years old; Caignard *et al.* 2021; Caignard *et al.* 2023). At these sites, budburst and LSF damage were monitored at the individual-tree scale, with an average of 532 trees per site. Both the occurrence and extent of LSF damage were recorded, the latter being available for 11 site-years. Daily temperature data for these sites were obtained from the nearest MétéoFrance meteorological stations between 1960 and 2021 (average distance of 12 km and elevation difference of 28 m; https://meteo.data.gouv.fr/).

The second source of data was the French Forest Health Department (DSF, https://agriculture.gouv.fr/actualite-en-sante-des-forets), which provided records from 289 oak sites. Among these, 36 continuous monitoring sites reported whether LSF damage occurred annually between 1997 and 2021 (25 years per site, totaling 900 site-years; 56 damage years and 844 non-damage years). For this source, information on the extent of LSF damage was available for 22 site-years. In addition, DSF archives included 253 more reports of LSF damage from non-continuous monitoring sites, which documented only occurrence but not non-occurrence or damage extent. Climate data for this source were obtained from the SAFRAN reanalysis at 8×8 km^2 spatial resolution for 1960–2021 (Vidal *et al.* 2010).

Together, these complementary sources provide a comprehensive dataset. We used the full dataset (1220 site-years, 304 sites) to validate model predictions of LSF occurrence, and the subset of site-years with extent data (33 site-years across both sources) to test model predictions of frost damage extent.

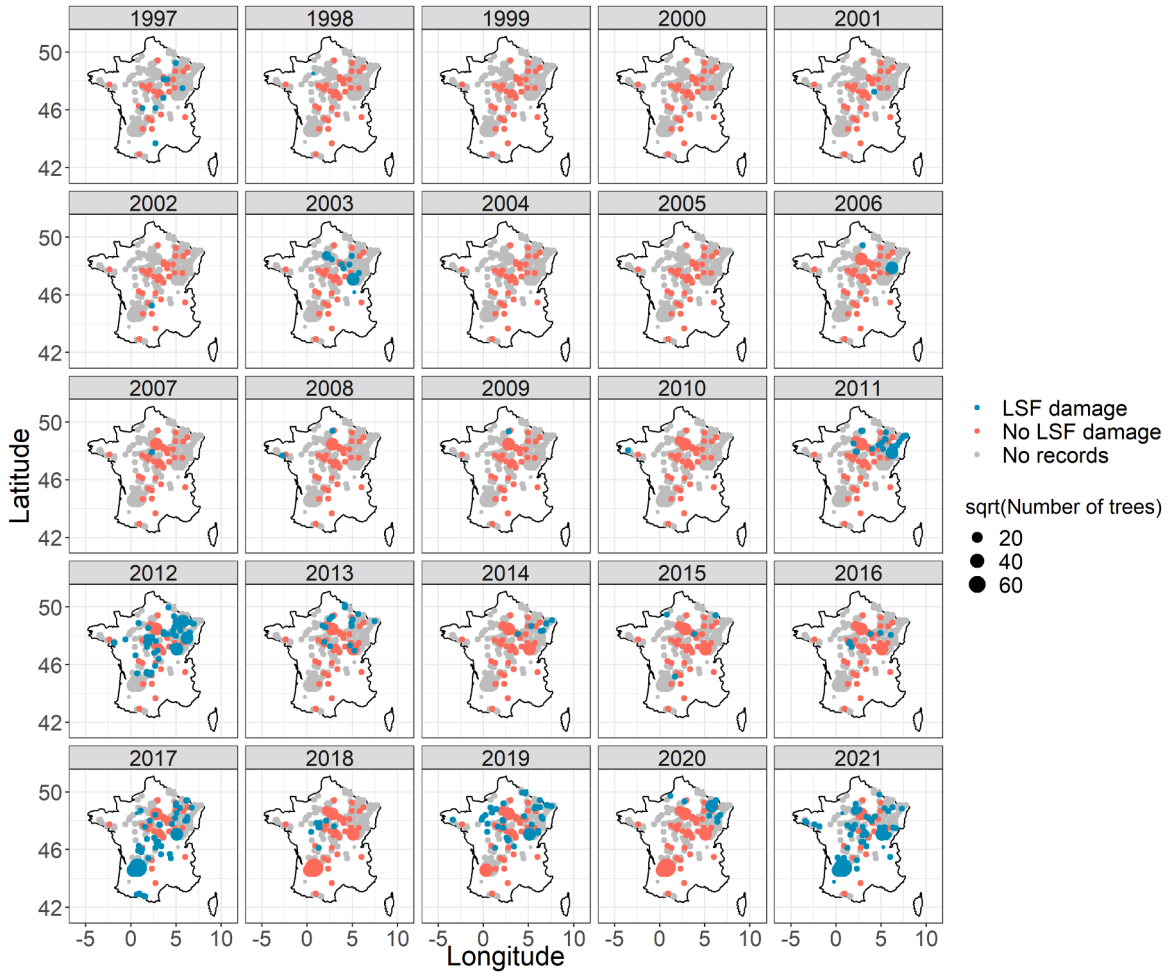

Fig. 1. Late spring frost (LSF) damage observations at 304 sites across France from 1997 to 2021. Each point represents one site-year observation. Blue points indicate the presence of LSF damage, red points indicate the absence of damage, and gray points indicate missing records for that particular year. Point size reflects the number of observed trees at each site.

2.2. Predicting late spring frost damage in tree populations

We simulated the damage caused by LSF using a model (FD_{WPV}) consisting of two modules: the first predicts the within-population variability (WPV) of the budburst date (Lin *et al.* 2024), while the second predicts the occurrence of frost damage for one tree when the temperature falls below a critical threshold (T_{frost}) during the vulnerability window of new leaves (Supplementary Figure 2). In this study, we specifically targeted frost events causing severe damage, characterized by the death of new leaves (Supplementary Figure 3), while excluding minor injuries like leaf edge curling or yellowing from the analysis.

2.2.1. Module 1: Within-population variability of budburst

The WPV module was constructed to predict the progress of budburst in tree populations (i.e., the percentage of trees having burst buds at a given date in a tree population) and was validated in a previous study (Lin *et al.* 2024). The WPV module was calibrated and validated using an extensive budburst dataset in oak populations. In this dataset, one tree was considered to have burst its buds when at least 50 % of the buds in the upper third of the crown presented leaves extending beyond the tip of the scales, which corresponded to stage BBCH 9 (Meier 1997).

At the 15 phenological monitoring sites that comprised both the frost damage and budburst observations (first data source described above), we were able to evaluate the ability of the WPV model to simulate the progress of budburst. Although the WPV model had been validated previously on an independent dataset, we re-evaluated it here to confirm its robustness and applicability to the larger, integrated dataset used in this study. The WPV model accurately predicted the timing of budburst with a root mean square error (RMSE) of 7.4 ± 1.7 days and the percentage of budburst progress with an RMSE of 25.2 ± 7.7 % (Supplementary Figure 4). The WPV model parameterization used here is identical to the original publication (Lin *et al.* 2024), as determined initially for the two oak populations in France. We are confident about the applicability of the WPV model at the DSF sites (second data source), although there are no phenological observations to directly evaluate the WPV model. Indeed, the WPV model performed well at the 15 phenological monitoring sites (first data source), which includes a temperature gradient (mean temperature in Jan.-May: 4-12 °C) that covers 98 % of the distribution of Jan.-May temperatures across the DSF sites (Supplementary Figure 5).

2.2.2. Module 2: T_{frost} and the vulnerability window of new leaves to frost

Tree tissue (e.g., leaves) can often resist temperatures colder than 0 °C (Vitasse *et al.* 2014; Zohner *et al.* 2020). Based on our observations, we defined T_{frost} as -3 °C for oak (cf. the Orsay and Barbeau oak populations in Supplementary Table 2), which is in line with previous studies (Eaton *et al.* 2016). Moreover, in our leaf frost observation dataset (see details below), the average absolute daily minimum air temperature (T_{min}) during the vulnerability window of leaves (i.e., 25 days after budburst; see below) was -3.3 °C (Supplementary Figure 6), which also supports the value chosen for T_{frost}. Based on the field observations (Supplementary Table 3) and results from the study of Liepe

(1993), we set the length of the vulnerability window of new leaves to frost to 25 days after budburst. This length is consistent with the results of Lenz et al. (2013), who showed that frost resistance barely changed in the 3 weeks after leaf unfolding for oak (see their Fig. 2). For the sake of model parsimony, we set a fixed length of 25 days for the vulnerability window of new leaves, bearing in mind that the maturation of leaves after budburst is modulated by temperature conditions (Davi *et al.* 2008), which would likewise modify the length of the vulnerability window. We also tested other vulnerable periods of 10, 15, 20, or 30 days (Supplementary Figure 7), but the main results did not change. Furthermore, predicting the extent of LSF damage was most accurate when using 25 days as the length of the vulnerability window (Fig. 3b, Supplementary Figure 7).

As mentioned above, temperature data were obtained from two sources, MétéoFrance on-site meteorological stations and SAFRAN reanalysis. Based on 6-hourly data produced by local meteorological stations and combined into an 8-km grid point, SAFRAN is known to overestimate the actual T_{min} (Supplementary Figure 8, Vidal *et al.* 2010). To compensate for this overestimation of T_{min} in the SAFRAN dataset, we set a different T_{frost} (-1 °C) for the sites using SAFRAN temperatures compared to -3 °C for the sites using temperature data from a meteorological station. We set the specific T_{frost} value (-1 °C) based on comparing the minimum temperatures recorded on frost days at sites with access to both SAFRAN temperatures and local meteorological station data (Supplementary Figure 9). Furthermore, we explored the use of a consistent temperature dataset by applying SAFRAN-derived temperatures to simulations across all 304 sites. However, this approach resulted in comparable but less accurate predictions (Supplementary Figure 10).

Most documented cases of frost damage in the first data source concerned mature oak trees in natural forest populations (i.e., 87 % of cases). However, it also included observations of LSF damage for young oak trees at the pole stage, located in two common gardens: at the Toulenne common garden, trees were 15 years old with an average height of 5.4 ± 2 m, while at the Pierroton common garden, trees were 6 years old with an average height of 0.7 ± 0.3 m. In the common gardens, the trees were shorter than in natural forests. The trees also experienced lower temperatures than those at the meteorological stations (Gril *et al.* 2023) due to the nighttime thermal inversion. Thus, specifically for these two sites, we set T_{frost} at a value of -1.2 °C (based on observations in common gardens) so that the model better simulated frost damage.

Due to the ability of the WPV model to predict the continuous progress of budburst in the population, our model predicted not only the possible occurrence of LSF damage but also the proportion of damaged trees, i.e., the extent of LSF damage in the population (Supplementary Figure 11). Our approach (FD_{WPV}) thus improves the previous LSF damage models (FD_{AVE}) (Liu *et al.* 2018; Meng *et al.* 2021), which assume that LSF damage occurs when temperatures are lower than a threshold (usually 0 °C) between the date of average budburst and the summer solstice (Supplementary Figure 11c).

2.3. *Evaluating the ability of FD_{WPV} to predict the frequency and extent of late spring frost damage in tree populations*

We used 1,220 site-year records of LSF occurrence, including both damage and non-damage years, from 304 sites to validate the FD_{WPV} predictions of LSF occurrence. Specifically, we predicted the continuous progress of budburst in the population. If the daily minimum temperature was below T_{frost} on a given day, we considered that the trees that had burst buds 25 days (i.e., corresponding to the leaf vulnerability window; see above) before the frost day would be damaged. This model allowed us to predict both the existence of LSF damage and the proportion of trees with potential damage (Supplementary Figure 11), a second novel feature of this model. To account for the substantial variation in the number of trees observed across sites, we used a weighted approach to calculate the root mean square error (RMSE) for LSF damage extent. This approach ensures that differences in tree counts are accurately reflected in the error calculation:

$$RMSE = \sqrt{\frac{\sum_{i=1}^{n}\left(\sqrt{num} \times \left(Extent_{obs,\ i} - Extent_{pred,\ i}\right)^2\right)}{\sum_{i=1}^{n}\sqrt{num}}}$$

Where *RMSE* represents the weighted root mean square error for LSF damage extent (in %), *num* is the number of trees observed on each site-year *i*, $Extent_{obs,\ i}$ is the observed LSF damage extent for site-year *i*, $Extent_{pred,i}$ is the predicted LSF damage extent for site-year *i* and *n* is the total number of site-years.

Moreover, we also evaluated the ability of FD_{AVE} to predict LSF damage with two values of T_{frost} (i.e., 0°C, which is often used in previous studies (Liu *et al.* 2018; Meng *et al.* 2021) and the same T_{frost} used in FD_{WPV}).

We evaluated the ability of the model to predict the occurrence and non-occurrence of LSF damage using the true skill statistic (TSS, Allouche *et al.* 2006). TSS ranges from -1 to 1, with the latter corresponding to a perfect prediction. TSS is thus calculated as follows:

$$TSS = sensitivity + specificity - 1$$

$$sensitivity = \frac{\text{Number of correctly predicted site} \sim \text{years with LSF damage}}{\text{All recorded site} \sim \text{years with LSF damage}}$$

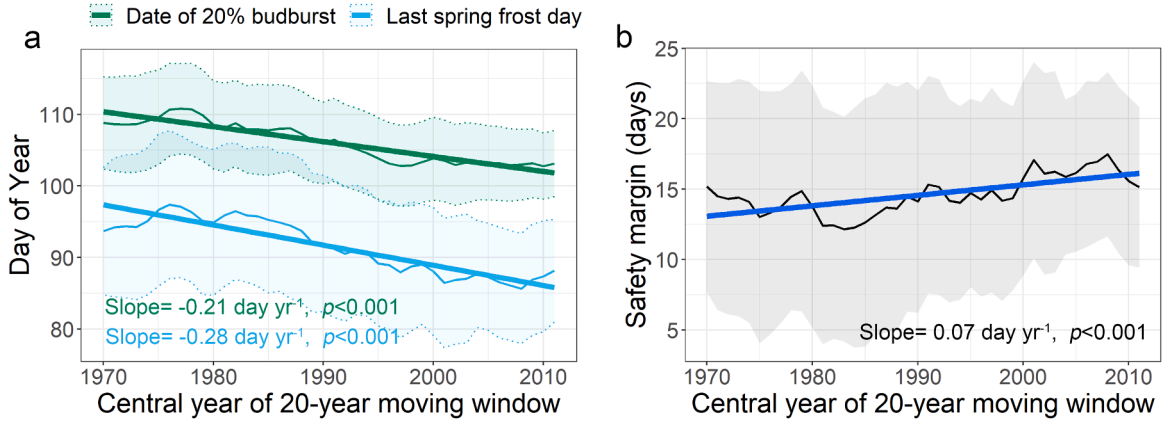

Fig. 2. Temporal trends in (a) budburst timing, last spring frost day, and (b) safety margin across 304 oak populations in France. The date of 20 % budburst represents the timing when 20 % of the trees in a population have burst buds, as simulated using the Within-Population Variability model for budburst. The last spring frost day is defined as the final day before the summer solstice with minimum temperatures (T_{min}) low enough to cause frost damage ($T_{min} < T_{frost}$). The safety margin represents the interval between the 20 % budburst date and the last spring frost day. Thin lines show the actual values, calculated with a 20-year moving window across the 304 populations, with shaded areas revealing the standard deviation across populations. Thick lines display fitted linear trends.

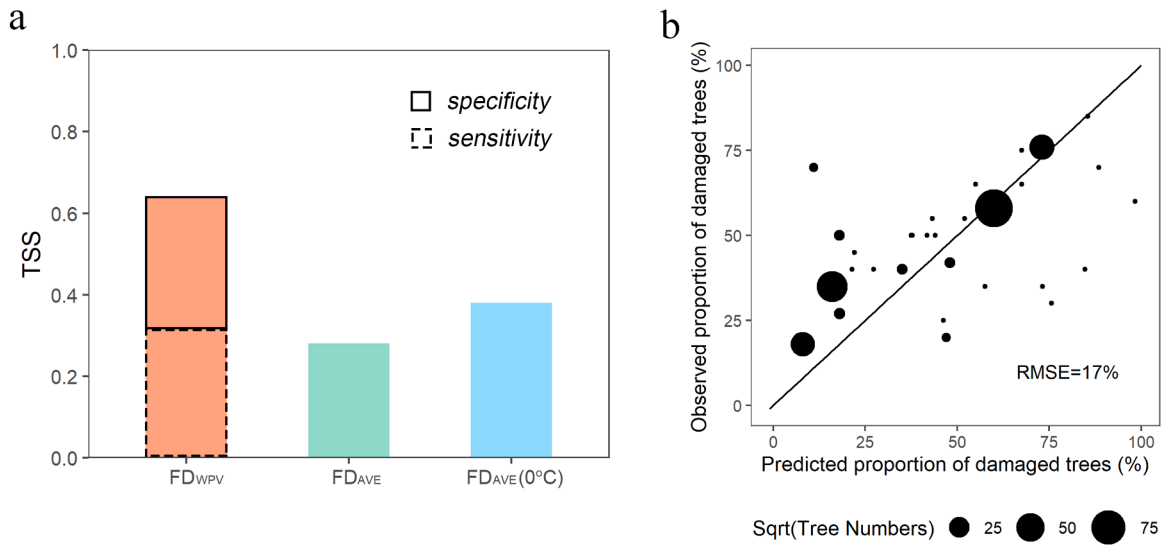

Fig. 3. Evaluation of frost damage models for predicting the occurrence (i.e., whether there is frost damage) and extent (i.e., percentage of trees in a population that are damaged by a given LSF event) of late spring frost (LSF) damage in the 304 oak populations examined. (a) Ability of the different models to predict the occurrence of LSF damage using True Skill Statistics (TSS) over the whole dataset (304 sites). Solid box is *sensitivity* which quantifies the model's ability to predict presences (i.e., years with LSF damage), and dashed box is *specificity* which quantifies the model's ability to predict absences (i.e., years with no LSF damage). "FD_{WPV}" is the new frost damage model introduced here based on the simulation of the within-population variability of budburst and a new-leaf vulnerability to frost window (see text). FD_{AVE} is a model that considers the average date of budburst as the start of the vulnerability window and uses the same threshold as FD_{WPV} for the damaging frost temperature. $FD_{AVE}(0°C)$ is otherwise similar to FD_{AVE}, but the value of $T_{frost} = 0°C$ is used. (b) Ability of the FD_{WPV} model to simulate the extent of LSF damage in oak populations. Point sizes are scaled with the number of observed trees.

$$specificity = \frac{\text{Number of correctly predicted site}\sim\text{years with no LSF damage}}{\text{All recorded site}\sim\text{years with no LSF damage}}$$

where *sensitivity* quantifies the model's ability to predict presences (i.e., years with LSF damage), and *specificity* quantifies the model's ability to predict absences (i.e., years with no LSF damage).

2.4. Calculating the trends of the frequency and extent of late spring frost damage in oak populations

The WPV model was designed to simulate the progress of budburst in tree populations (from 0 % to 100 % budburst). However, the model was calibrated and validated mainly using data that document the budburst dynamics after 20 % budburst (Lin *et al.* 2024). Thus, we focused our analyses on the LSF damage that occurred after 20 % of trees had burst buds in the population. Given that LSF damage is a relatively rare event, we adopted a moving window method to detect the successive temporal changes in the frequency and extent of LSF damage. We computed the frequency of LSF damage (i.e., the proportion of years with LSF damage) and the extent of LSF damage (i.e., percentage of trees in a population damaged by a given LSF event) in the population. Within each moving window, the extent of LSF damage is only considered for the years with LSF damage by averaging the proportion of damaged trees in the population in the years with frost damage while excluding the years without frost damage.

Given the 61 years (1961-2021) of simulation results in our study, we used a 20-year moving window approach. Still, for window sizes between 15 and 35 years, the results were qualitatively similar (Supplementary Figure 12). Moreover, Mann–Kendall trend analysis was also used to test for the magnitude and direction of temporal changes of LSF damage (Mann 1945; Kendall 1948; Zohner *et al.* 2020).

2.5. Evaluating the spatial variability of the late spring frost damage in oak population

To assess the spatial variability of LSF damage within oak populations, we analyzed the proportion of years with LSF damage and the average extent of LSF damage across 61 years. To minimize the impact of single, high-extent LSF damage, we included only sites with LSF damage occurrences in at least three different years over this period. Additionally, Pearson correlation analyses were performed to examine relationships between the proportion of years with LSF damage and the average LSF damage extent with geographic and environmental factors, including longitude, latitude, elevation, and the site's mean annual temperature. The site's mean annual temperature was selected as it reflects the overall climatic and thermal conditions of each site, making it suitable for examining spatial variability among sites.

2.6. Analyzing the relation between the frequency and extent of late spring frost damage and environmental factors

We defined the *safety margin* as the duration between the date of budburst predicted by the WPV model and the last spring frost following Lenz et al. (2013):

Safety margin (in days) = DoY (20 % of trees have burst buds) - DoY (last spring frost day)

The last spring frost day is the last day that occurs before the summer solstice with a daily minimum temperature below T_{frost}. To be consistent with calculating the frequency and extent of LSF damage, we also used a moving window to calculate the trend of safety margin with a 20-year window size. Specifically, we calculated the mean safety margin across the 304 study sites within each moving window and then used linear regression to obtain the trend of safety margin over the past six decades. We used linear regression to analyze the correlation between the trend of safety margin and the trends of the frequency and extent of LSF damage in the population. The same approach was applied to analyze the temporal trends in the timing of 20 % budburst and the last

spring frost day. This consistent methodology ensured comparability across variables and provided a robust framework for identifying long-term patterns and correlations.

Pearson correlation analysis was used to analyze the relation between the frequency and extent of LSF damage in the population on the one hand and geographical and environmental factors on the other (i.e., longitude, latitude, altitude, trend of mean temperature in first five months of the year over the 1961-2021 period, trend of last spring frost day, and trend of the date at which 20 % budburst occurs). Moreover, we also analyzed the correlation between the frequency and extent of LSF damage in a population using Pearson correlation analysis.

All simulations and statistical analyses were carried out with R statistical software v.4.0.3 (R Core Team 2023).

3. Results

3.1. Late spring frost damage

Fig. 1 shows the spatial and temporal distribution of LSF damage observed across oak populations in France from 1997 to 2021. Frost occurrences varied spatially, with more frequent events in northern and eastern regions, particularly in 2003, 2006, 2011, 2013, and 2020. In some years, such as 2012, 2017, and 2021, frost events were widespread, affecting many locations, whereas in most other years, only a few sites recorded frost damage.

3.2. Temporal changes in budburst date, last spring frost day, and safety margin

Over 1961-2021, the date of 20 % budburst simulated by the within-population variability model in oak populations showed a significant advancing trend of 2.1 days per decade ($p < 0.001$, Fig. 2a). Concurrently, the timing of the last spring frost day, defined as the final day before the summer solstice when daily minimum temperatures are low enough to cause frost damage, advanced by 2.8 days per decade ($p < 0.001$, Fig. 2a). Consequently, the safety margin of oak populations, representing the interval between the 20 % budburst date and the last spring frost day, exhibited a significant increasing trend over time ($p < 0.001$, Fig. 2b).

3.3. Validation of the novel late spring frost damage model with extensive frost damage data

Our model (i.e., FD_{WPV} model) simulating the within-population variations of frost damage was supported by the LSF damage records taken from 304 oak sites. This was confirmed by the higher value of the *true skill statistic* (TSS=0.64, Fig. 3) compared with the previous modeling approach (a model called FD_{AVE}), which assumed that LSF damage occurs when the minimum temperature drops below a certain threshold temperature between the average date of budburst in the population and the summer solstice (Liu *et al.* 2018; Meng *et al.* 2021). The model demonstrated a well-balanced discriminative capacity in TSS optimization, achieving a *sensitivity* of 0.80 and a *specificity* of 0.84. This indicates a comparable accuracy in identifying both years with LSF damage and years without damage. Importantly, contrary to FD_{AVE}, the FD_{WPV} model was able to predict the extent of LSF damage (i.e., the percentage of trees actually damaged by a given LSF event), too, with an RMSE of 17 % (Fig. 3).

3.4. Overall decrease in the frequency and extent of late spring frost damage over time

The average frequency of LSF damage (i.e., probability of LSF in a given year) was generally in the range of two to five events in 20 years (i.e., probability of 11 % to 25 %; Fig. 4a), and the average extent of LSF damage (i.e., percentage of trees in a population damaged by a given LSF event) in the population, calculated for the years when LSF damage occurred, ranged from 43 % to 58 % in the past six decades across the 304 sites examined (Fig. 4b). Under ongoing climate warming from 1961 to 2021 (Supplementary Figure 13), the frequency and extent of LSF damage in oak populations showed a general significant decreasing trend at rates of 0.22 % $year^{-1}$ and 0.34 % $year^{-1}$, respectively, based on the moving window approach (using a 20-year window size) ($p < 0.05$, Fig. 4). This result is consistent with an overall increasing trend of the safety margin in the past six decades (Fig. 2). Moreover, the Mann–Kendall trend analysis also showed a decreasing trend in the frequency and extent of LSF damage (Supplementary Table 4). Although we used linear regression to simplify the analysis and highlighted a general downward trend of LSF damage frequency during the past six

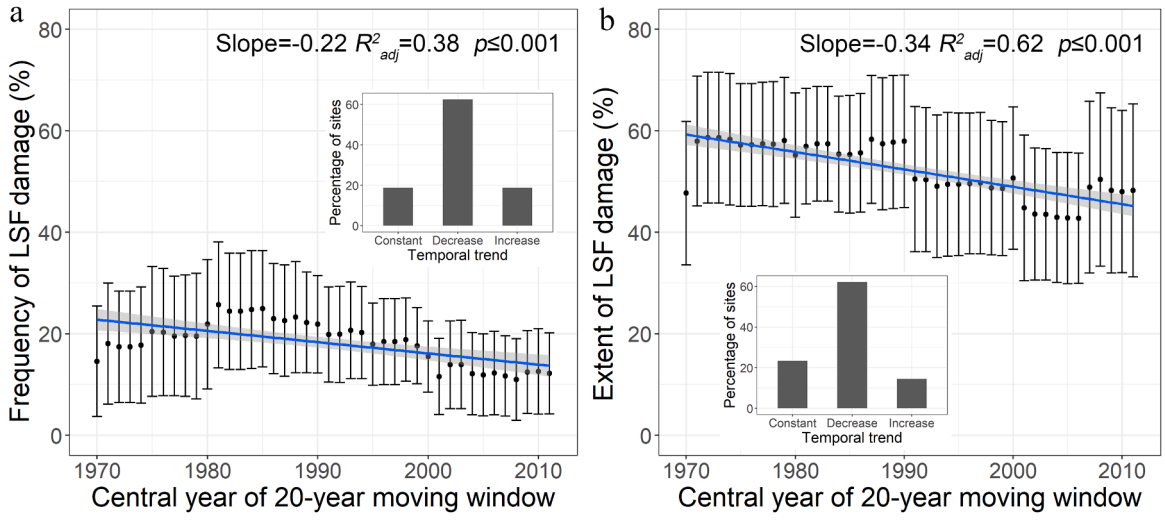

Fig. 4. Temporal trend of the frequency (a) and extent (b) of late spring frost (LSF) damage in the 304 oak populations examined, as simulated by the FD_{WPV} model. FD_{WPV} model is the new frost damage model introduced here based on the simulation of the within-population variability of budburst and a new-leaf vulnerability to frost window. (a) LSF damage frequency is calculated as the proportion of years with LSF damage occurring within a 20-year moving window. (b) LSF damage extent is calculated as the mean of the percentage of damaged trees within a 20-year moving window (considering only years when LSF occurs). Each point is the mean of the frequency or extent of LSF damage across the 304 sites, while the error bar is the standard deviation across the 304 sites. The fitted blue lines highlight the linear trends over time. The gray shaded area indicates the 95 % confidence interval. The insets represent the percentage of sites with different trends of the frequency and extent of LSF damage over time.

decades, we observed that this trend of LSF damage frequency varied over time. For instance, the trend of LSF damage frequency increased before the 1980 s ($p < 0.01$, Fig. 4a).

3.5. Spatial variability of the frequency and extent of late spring frost damage in oak populations

Our findings reveal substantial spatial variability in LSF damage. From 1961-2021, the proportion of years with LSF damage was higher, and the average extent of LSF damage was greater at sites located further east (Fig. 5). Additionally, the frequency of LSF damages over the past 61 years showed a significant negative correlation with the site's mean annual temperature ($p < 0.05$), indicating that sites with higher temperatures experienced LSF damage less frequently. However, no significant relationship was found between the frequency of LSF damages and either elevation or latitude. Conversely, the average extent of LSF damage over the past 61 years was significantly positively correlated with the site's mean annual temperature ($p < 0.05$), suggesting that warmer sites, such as those at lower elevations ($p < 0.05$) and latitudes ($p = 0.07$), see a larger proportion of trees damaged when frost damage occurs.

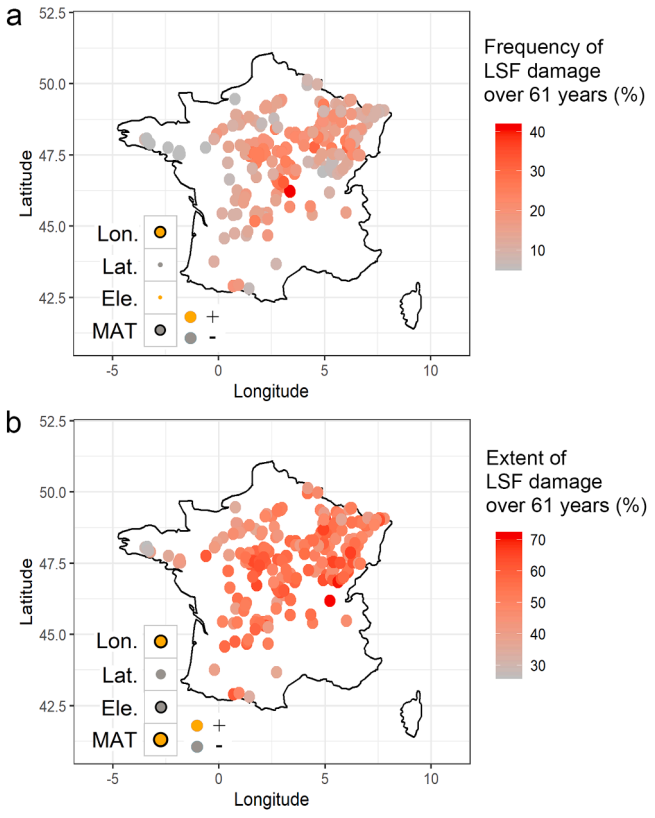

Fig. 5. Spatial variability of late spring frost (LSF) damage in oak populations over the past 61 years in France. (a) Frequency of LSF damage (i.e. proportion of years with LSF damage) over 61 years (1961-2021). (b) Average extent (i.e., percentage of damaged trees when LSF occurs) of LSF damage across sites with at least three years of recorded LSF events, where color gradients indicate the average extent over the 61-year period. Insets depict correlations of the frequency (a) and extent (b) with longitude (Lon.), latitude (Lat.), elevation (Ele.), and the sites' mean annual temperature (MAT) calculated over 1961-2021. In the insets, the size of the dots relates to value of the correlation coefficient (with smaller dots illustrating $r = 0.02$ and larger dots illustrating $r = 0.22$). Orange and gray indicate positive and negative correlations, respectively. Bold black circles indicate significant correlations ($p < 0.05$).

3.6. Different trends of late spring frost damage across sites

Temporal trends in LSF damage were not uniform for oak populations across France (Fig. 6a, b). Indeed, 63 % of sites showed a decreasing trend in LSF damage frequency (i.e., negative slope with respect to time, with $p < 0.05$, Fig. 4 insets), whereas 18.5 % of sites had an increasing trend (i.e., positive slope with respect to time, with $p < 0.05$) and 18.5 % showed no trend (i.e., slope with respect to time not significantly different from zero, with $p > 0.05$). We found that the variability in the trend of LSF damage frequency among sites was largely explained by the variability of the trend of safety margin (Fig. 6c, noting that 55 % of sites showed an increasing trend of safety margin, 31 % of sites showed a decreasing trend, and 14 % no trend; Supplementary Figure 14b). At sites where the safety margin became larger with time, the LSF damage frequency tended to decrease ($p < 0.001$, $R^2_{adj} = 0.56$, Figs. 6c and 7a). Moreover, we found that LSF damage also became less frequent over time for populations at a lower elevation or a higher longitude (i.e., for populations located eastwards, $p < 0.05$, Fig. 7a and Supplementary Figure 15). Interestingly, the correlation between the trends of budburst and LSF damage frequency was positive, indicating that, counterintuitively, the trend toward earlier budburst was associated with less frequent LSF damage (Fig. 7a). When considering the trend of the extent of LSF damage, we observed that, as expected, it decreased as the safety margin became larger with time (Fig. 6d). However, this correlation was less pronounced ($p < 0.001$, $R^2_{adj} = 0.03$, Fig. 6d) than the correlation between the trends of safety margin and LSF damage frequency (Fig. 6c). Oak populations located at lower elevations experienced a declining trend in terms of the extent of LSF damage. However, contrary to the frequency of LSF damage, the trend of the extent of LSF damage increased eastwards ($p < 0.05$, Fig. 7a). Importantly, we found no significant correlation between the trends of the frequency and extent of LSF damage across all sites ($p > 0.05$, Fig. 7b), with 36 % of sites exhibiting opposing trends between frequency and extent.

4. Discussion

The findings of studies published to date on the changes in the frequency of LSF damage are inconsistent, with some reporting an overall upward trend and others a generally decreasing or no trend in terms of the frequency of LSF damage over the past few decades (summarized in Supplementary Table 5, Hänninen 1991; Scheifinger *et al.* 2003; Rigby & Porporato 2008; Bennie *et al.* 2010; Augspurger 2013; Morin & Chuine 2014; Bigler & Bugmann 2018; Liu *et al.* 2018; Vitasse *et al.* 2018; Zohner *et al.* 2020). However, most studies report theoretical results not validated by direct observations of frost damage on leaves. Because LSF events do not occur at regular intervals and are unevenly distributed in time and space, the time series of observed plant damage due to LSF events are sparse. Consequently, most studies rely on proxies for actual LSF events (e.g., FD_{AVE}). Furthermore, none of these studies addresses the extent of frost damage (i.e., percentage of trees in a population damaged by a given LSF event) within tree populations. To our knowledge, despite extensive research on the impacts of LSF damage on various species in previous studies (Supplementary Table 5), no quantitative results regarding the long-term damage to oaks from LSF have been provided so far in the literature. In the present study, we developed a new model based on the direct observation of LSF, which showed a general decrease in LSF frequency in oak populations over the past six decades in France. Behind this general trend, we showed region-specific variability in the frequency of LSF damage (Zohner *et al.* 2020). Previous studies have documented region-specific variability in LSF damage (Hufkens *et al.* 2012; Liu *et al.* 2018; Chamberlain *et al.* 2019). However, these studies have several limitations. For instance, Hufkens et al. (2012) validated their results using remote sensing data of LSF damage. However, their remote sensing data only cover a short period (5 years). In other studies, long-term trends of LSF damage were studied at the

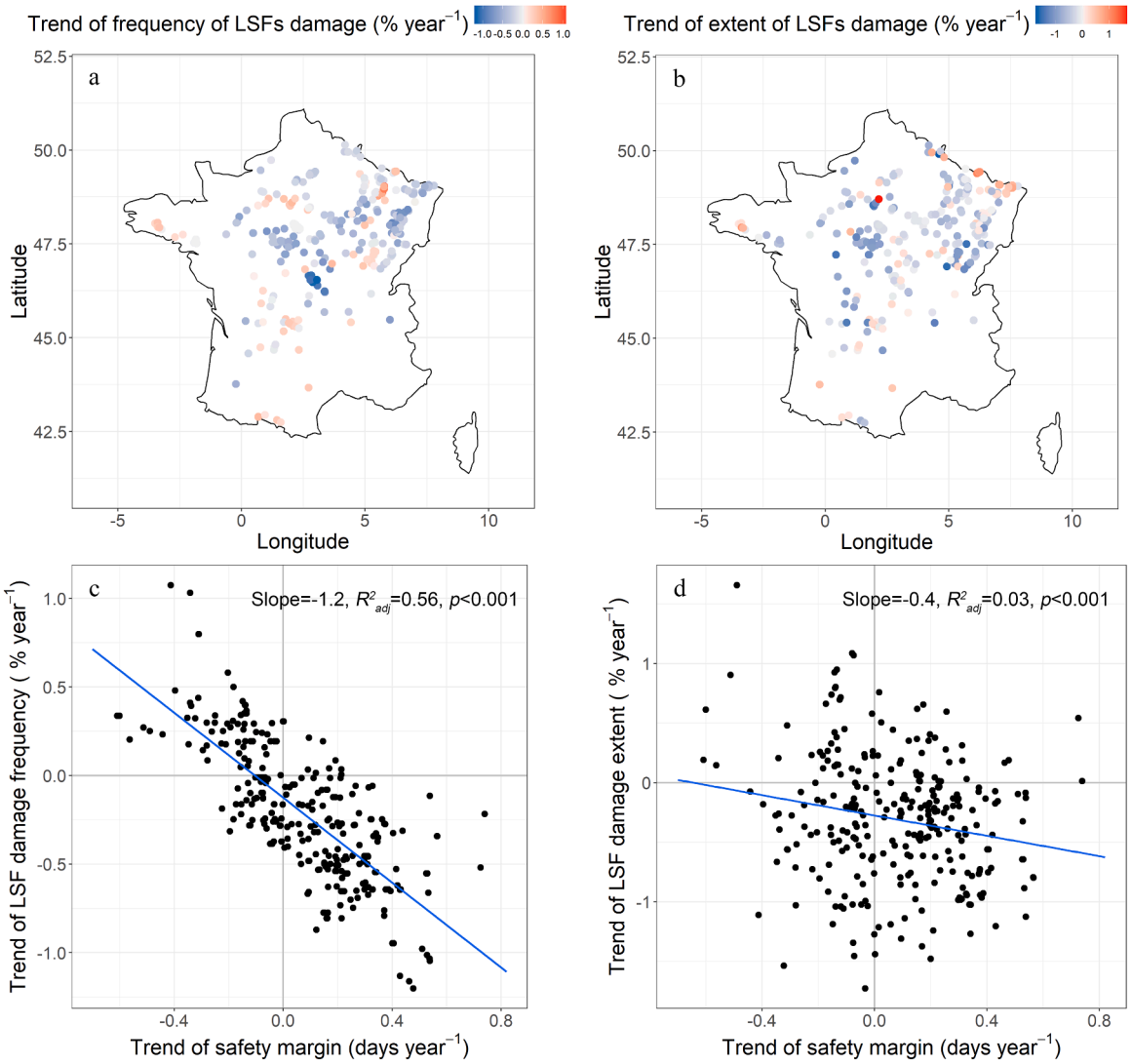

Fig. 6. Spatial representation of the trends of the frequency (a) and extent (b) of late spring frost (LSF) damage and the relation between the trends of safety margin and frequency (c) and the trends of safety margin and extent (d) of LSF damage in the 304 oak populations examined. In (a) and (c), the "trend of the frequency of LSF damage" indicates the temporal change in the proportion of years with LSF damage within a 20-year moving window. In (b) and (d) the "trend of the extent of LSF damage" indicates the temporal change in the mean extent of LSF damage, i.e., the mean percent of damaged trees, when LSF occurs, within a 20-year window. The trend of safety margin (i.e., the time interval between the date at which 20 % of trees have burst buds and the last spring frost day) is a temporal change of the mean safety margin within a 20-year window. Each point represents one site. In (a) and (b), the color gradient indicates the magnitude of the trend.

continental level by inference through a combination of phenological changes and climate change (Zohner *et al.* 2020). These studies suffer from a lack of observational validation and cannot provide precise species-specific results. Our study provided representative results for oak populations based on the validation of long-term and large-scale observation records, thus allowing us to accurately evaluate the change in LSF damage with climate warming.

4.1. Temporal and spatial change of late spring frost damage frequency across oak populations

In general, we found that 63 % of sites showed a downward trend in the frequency of LSF damage, leading to a significant decrease in LSF damage to populations over the 1961-2021 period examined in our study. This is consistent with the results of Scheifinger et al. (2003), who showed that LSF damage to plants at 50 stations in Central Europe was lower in the 1990s compared with the previous decades. However, these findings are contrary to studies pointing to trends of greater LSF damage in the United States in 1889-1992 (Augspurger 2013) and at high elevations (>800 m.a.s.l.) in Switzerland in 1975-2016 (Vitasse *et al.* 2018). Such discrepancies likely reflect differences in site characteristics, environmental conditions, and species-specific budburst strategies shaped by long-term adaptation (Zohner *et al.* 2020), as well as differences in the periods examined (Bigler & Bugmann 2018).

Contrary to previous findings (Dantec *et al.* 2015), we did not detect a significantly higher proportion of frost years at high elevations, possibly due to the limited number of high-elevation sites in our dataset (Supplementary Figure 16) and the broad regional scope of our analysis, which may dilute elevation-related effects. Nevertheless, our analysis shows that the temporal trend of LSF damage frequency increased significantly with elevation, consistent with previous findings that climate warming has increased the likelihood of LSF damage at higher elevations, while little to no trend is evident at lower elevations (Vitasse *et al.* 2018). This pattern can be explained by the stronger temporal decline of the safety margin at higher elevations, where the advance of budburst outpaced that of the last spring frost day, resulting in an amplified increase in LSF damage probability over time (Vitasse *et al.* 2018). In addition, our results showed that the proportion of frost years

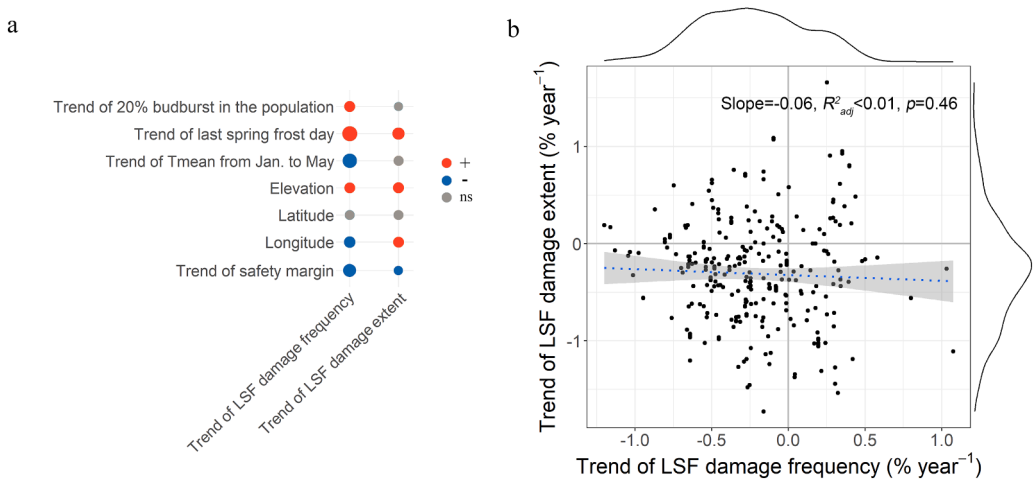

Fig. 7. Relation between environmental factors and the trends of the frequency and extent of late spring frost (LSF) damage. The "trend of LSF damage frequency" indicates the temporal change of the proportion of years with LSF damage within a 20-year moving window. The "trend of LSF damage extent" indicates the temporal change of the mean extent of LSF damage within a 20-year window. (a) Correlation between the trends of the frequency and extent of LSF damage and the trends of environmental factors over time. The trend of safety margin (i.e., the time interval between the date at which 20 % of trees have burst buds and the last spring frost day) is the temporal change of the mean safety margin within a 20-year window. The size of the dots indicates the correlation coefficient (with smaller dots illustrating r = 0.03 and larger dots illustrating r = 0.75). Red and blue indicate significant positive and negative correlations ($p < 0.05$), respectively, while gray indicates non-significant correlations. (b) Correlation between the trends of frequency and extent of LSF damage over time. The fitted dotted line highlights the relation between the trends of the frequency and extent of LSF damage in the population. The shaded area shows the 95 % confidence interval. The curves above and to the right of the panel indicate the density of the trends of the frequency and extent of LSF damage, respectively. Each point represents one site.

increased eastward with distance from the coast, likely because warm ocean currents reduce the risk of LSF damage in coastal regions (Zohner et al. 2020). Interestingly, eastern regions also showed a stronger decline in damage frequency over time (Ma et al., 2019), which may reflect stronger land-based warming relative to coastal areas (Dommenget, 2009).

Our study is the first to use extensive records of LSF damage to make inferences about LSF damage trends. Moreover, we confirmed a strong correlation between trends in LSF damage frequency and the safety margin, thereby empirically validating the latter as a reflection of the probability of LSF damage, which has been postulated in previous studies (Lenz *et al.* 2013; Vitasse *et al.* 2018; Chamberlain *et al.* 2019) but not yet verified. We further tested the trend of LSF damage frequency using the FD_{AVE} model from previous studies, which assumes that LSF damage occurs when temperatures fall below a threshold (usually 0°C) between the average budburst date and summer solstice (Liu *et al.* 2018; Meng *et al.* 2021). This model also confirmed a decreasing trend of LSF damage frequency over time (Supplementary Figure 17).

A common view is that earlier budburst leads to more frequent LSF damage (Hänninen 1991; Liu *et al.* 2018; Meng *et al.* 2021). However, we found the opposite phenomenon in our study, namely that the trend of earlier budburst was associated with a trend of a lower frequency of LSF damage (Fig. 7a). This may be explained by the fact that the last spring frost day also advanced in the context of climate warming but at a faster rate than the advancement of budburst. Indeed, partial correlation analysis revealed that when controlling for the effect of warming temperature, earlier budburst was, as expected, associated with a higher probability of LSF damage (partial correlation of budburst with LSF frequency while controlling for spring temperature was -0.13, $p < 0.05$). This phenomenon is further supported by the spatial variability in LSF damage, which shows a significant negative relationship between the proportion of frost years and the sites' mean annual temperature ($p < 0.05$, Fig. 5). Warmer sites exhibit a lower likelihood of LSF damage. In the 304 oak populations examined, earlier budburst is thus generally associated with a lower risk of LSF damage, with probable benefits for growth and productivity.

4.2. Temporal and spatial change of late spring frost damage extent across oak populations

Despite the wealth of studies on the frequency of LSF damage, very few focus on the extent of LSF damage in a tree population (Hufkens *et al.* 2012; Nolè *et al.* 2018), leaving an important gap in understanding LSF impacts. Our model simulations over the past 61 years suggest substantial spatial heterogeneity in the average extent of LSF damage. Warmer sites tend to exhibit a higher average extent of LSF damage, as earlier budburst induced by warmer conditions increased the proportion of trees exposed to frost events. Interestingly, although cooler, eastern sites show a higher average extent of LSF damage than western sites, likely due to the moderating influence of the nearby ocean, which reduces LSF damage extent near the coast. Importantly, we found that temporal changes in the extent of LSF damage in tree populations do not consistently align with changes in LSF damage frequency. Although climate warming tends to reduce the frequency of frost damage years, it also advances budburst, and late frost events still occur (Supplementary Figure 18), so the extent of damage does not necessarily mirror the decline in frequency. Thus, assessing frequency alone underestimates the threat posed by LSF damage, and a comprehensive evaluation requires considering both frequency and extent to capture the full risk to tree populations.

Additionally, the daily minimum temperature from budburst until mid-July (Hänninen 1991, 2016; Ma *et al.* 2019) is commonly used to assess the "severity" of LSF damages. Our findings show that changes in LSF damage severity varies among sites with climate warming: 78 % of sites show no significant trend, 10 % show a significant decline, and 12 % show a significant increase (Supplementary Figure 19). However, similar to previous studies (Hänninen 1991, 2016; Ma *et al.* 2019), our research lacks field observations to directly validate the prediction of LSF damage severity. In contrast to LSF damage severity, we used a novel frost damage model (i.e., FD_{WPV}) in this study to simulate the frequency and extent of LSF damage in French oak populations over the past six decades. Our model was validated using long-term LSF damage records, revealing high predictive accuracy for LSF damage frequency and extent. It is important to note that the extent metric specifically considers frost events causing new leaf mortality, reflecting severe LSF

damage and highlighting within-population damage variability. Therefore, we conclude that frequency and extent jointly comprehensively assess frost impact in tree populations.

Our study evaluates changes in LSF damage to oak populations over the past 61 years from both frequency and extent perspectives. Against the backdrop of global climate change, assessing frost risk through damage extent provides a novel viewpoint, as the weak correlation between frequency and extent underscores the need to consider both metrics. This dual approach offers a more comprehensive ecological and economic understanding of LSF damage risk (Lamichhane 2021) and could inform forestry and insurance policy decisions. Such a multifaceted assessment framework is essential for accurately evaluating frost risk to tree populations in a warming climate.

Data availability

The LSF data supporting the validation of the FD_{WPV} model are available at https://doi.org/10.5281/zenodo.17291255. Budburst data from phenological monitoring sites are available at http://www1.onf.fr/renecofor/@@index.html. Temperature data (1960–2021) were obtained from the nearest Météo France meteorological stations for phenology sites and from SAFRAN reanalysis at 8×8 km^2 resolution for DSF sites. Both temperature datasets are available from https://meteo.data.gouv.fr/.

Code availability

The codes used to generate the results in this study are available on Zenodo at https://doi.org/10.5281/zenodo.17168355

CRediT authorship contribution statement

Jianhong Lin: Conceptualization, Methodology, Formal analysis, Investigation, Writing – original draft. **Nicolas Delpierre:** Conceptualization, Supervision, Methodology, Investigation, Data curation, Writing – review & editing. **Fabien Caroulle:** Data curation, Writing – review & editing. **Sebastien Cecchini:** Data curation, Writing – review & editing. **Vincent Badeau:** Writing – review & editing. **Thomas Caignard:** Investigation, Writing – review & editing. **Daniel Berveiller:** Writing – review & editing. **Sylvain Delzon:** Writing – review & editing. **Heikki Hänninen:** Writing – review & editing. **Antoine Kremer:** Writing – review & editing. **Annette Menzel:** Writing – review & editing. **Alexandre Morfin:** Investigation, Writing – review & editing. **Julien Parmentier:** Investigation, Writing – review & editing. **Gaëlle Vincent:** Investigation, Writing – review & editing. **Rui Zhang:** Writing – review & editing. **Cyrille Rathgeber:** Writing – review & editing.

Declaration of competing interest

The authors declare that they have no known competing financial interests or personal relationships that could have appeared to influence the work reported in this paper.

Acknowledgements

We thank the Office National des Forêts, through the RENECOFOR network team, and the French ministry for Agriculture, through the Département Santé des Forêts, for coordinating and providing phenological and frost damage data. This paper builds on the thousands of hours of fieldwork done by the ONF foresters and DSF agents to collect data. We most sincerely thank them for their work. We thank MétéoFrance for producing and providing access to the SAFRAN data. We thank Isabelle Chuine and Sergio Rossi for their comments, which contributed to improving the manuscript. We further thank two anonymous reviewers whose comments helped improve the paper. This work was made possible by public fundings from the French Ministère de l'enseignement supérieur et de la recherche and Ministère de l'Agriculture. It was further supported by the China Scholarship Council (202008330320).

Supplementary materials

Supplementary material associated with this article can be found, in the online version, at doi:10.1016/j.agrformet.2025.110927.

References

Allouche, O., Tsoar, A., Kadmon, R., 2006. Assessing the accuracy of species distribution models: prevalence, kappa and the true skill statistic (TSS). J. Appl. Ecol. 43, 1223–1232.
Augspurger, C.K., 2013. Reconstructing patterns of temperature, phenology, and frost damage over 124 years: spring damage risk is increasing. Ecology 94, 41–50.
Bacilieri, R., Ducousso, A., Kremer, A., 1995. Genetic, morphological, ecological and phenological differentiation between *Quercus petraea* (Matt.) Liebl. and *Quercus robur* L. in a mixed stand of northwest of France. Silvae Genet. 44, 1–10.
Bennie, J., Kubin, E., Wiltshire, A., Huntley, B., Baxter, R., 2010. Predicting spatial and temporal patterns of bud-burst and spring frost risk in north-west Europe: the implications of local adaptation to climate. Glob. Change Biol. 16, 1503–1514.
Bigler, C., Bugmann, H., 2018. Climate-induced shifts in leaf unfolding and frost risk of European trees and shrubs. Sci. Rep. 8, 9865.
Caignard, T., Kremer, A., Bouteiller, X.P., Parmentier, J., Louvet, J.M., Venner, S., et al., 2021. Counter-gradient variation of reproductive effort in a widely distributed temperate oak. Funct. Ecol. 35, 1745–1755.
Caignard, T., Truffaut, L., Delzon, S., Dencausse, B., Lecacheux, L., Torres-Ruiz, J.M., et al., 2023. Fluctuating selection and rapid evolution of oaks during recent climatic transitions. Plants People Planet 6, 221–237.
Chamberlain, C.J., Cook, B.I., de Cortazar-Atauri, I.G., Wolkovich, E.M., 2019. Rethinking false spring risk. Glob. Change Biol. 25, 2209–2220.
Chuine, I., 2010. Why does phenology drive species distribution? Philos. Trans. R. Soc. B-Biol. Sci. 365, 3149–3160.
Dantec, C.F., Ducasse, H., Capdevielle, X., Fabreguettes, O., Delzon, S., Desprez-Loustau, M.L., 2015. Escape of spring frost and disease through phenological variations in oak populations along elevation gradients. J. Ecol. 103, 1044–1056.
Davi, H., Barbaroux, C., Dufrene, E., Francois, C., Montpied, P., Brea, N., et al., 2008. Modelling leaf mass per area in forest canopy as affected by prevailing radiation conditions. Ecol. Model. 211, 339–349.
Delpierre, N., Guillemot, J., Dufrene, E., Cecchini, S., Nicolas, M., 2017. Tree phenological ranks repeat from year to year and correlate with growth in temperate deciduous forests. Agric. For. Meteorol. 234, 1–10.
Denechere, R., Delpierre, N., Apostol, E.N., Berveiller, D., Bonne, F., Cole, E., et al., 2021. The within-population variability of leaf spring and autumn phenology is influenced by temperature in temperate deciduous trees. Int. J. Biometeorol. 65, 369–379.
Dittmar, C., Fricke, W., Elling, W., 2006. Impact of late frost events on radial growth of common beech (*Fagus sylvatica* L.) in Southern Germany. Eur. J. For. Res. 125, 249–259.
Dommenget, D., 2009. The ocean's role in continental climate variability and change. J. Clim. 22 (18), 4939–4952.
Eaton, E., Caudullo, G., Oliveira, S., De Rigo, D.J.E.A.o.F.T.S.P.P.O.o.t.E.U., 2016. *Quercus robur* and *Quercus petraea* in Europe: distribution, habitat, usage and threats. Eur. Atlas For. Tree Species 14, 160–163.
Faust, E., Herbold, J., 2018. Spring frost losses and climate change — not a contradiction in terms. https://www.munichre.com/topics-online/en/climate-change-and-natural-disasters/climate-change/springfrost-losses-climate-change-2018.html. Last accessed 1-8-2023.
Gril, E., Spicher, F., Greiser, C., Ashcroft, M.B., Pincebourde, S., Durrieu, S., et al., 2023. Slope and equilibrium: a parsimonious and flexible approach to model microclimate. Methods Ecol. Evol. n/a.
Gu, L., Hanson, P.J., Post, W.M., Kaiser, D.P., Yang, B., Nemani, R., et al., 2008. The 2007 eastern US spring freeze: Increased cold damage in a warming world? Bioscience 58, 253–262.
Hänninen, H., 1991. Does climatic warming increase the risk of frost damage in northern trees? Plant Cell Environ. 14, 449–454.
Hänninen, H., 2016. Boreal and temperate trees in a changing climate: Modelling the ecophysiology of seasonality. Springer Science +Business Media, Dordrecht.
Hufkens, K., Friedl, M.A., Keenan, T.F., Sonnentag, O., Bailey, A., O'Keefe, J., et al., 2012. Ecological impacts of a widespread frost event following early spring leaf-out. Glob. Change Biol. 18, 2365–2377.
Kendall, M.G. (1948). Rank correlation methods.
Lamichhane, J.R., 2021. Rising risks of late-spring frosts in a changing climate. Nat. Clim. Change 11, 554–555.
Lebourgeois, F., Pierrat, J.C., Perez, V., Piedallu, C., Cecchini, S., Ulrich, E., 2008. Déterminisme de la phénologie des forêts tempérées françaises: étude sur les peuplements du réseau RENECOFOR. Rev. For. Fr. 60, 323–343.
Lenz, A., Hoch, G., Vitasse, Y., Korner, C., 2013. European deciduous trees exhibit similar safety margins against damage by spring freeze events along elevational gradients. New Phytol. 200, 1166–1175.
Liepe, K., 1993. Growth-chamber trial on frost hardiness and field trial on flushing of sessile oak (*Quercus-Petraea* Liebl). Ann. Sci. For. 50 (Supplement 1), S208–S214. *199*350.

Lin, J., Berveiller, D., François, C., Hänninen, H., Morfin, A., Vincent, G., et al., 2024. A model of the within-population variability of budburst in forest trees. Geosci. Model Dev. 17, 865–879.
Liu, Q., Piao, S., Janssens, I.A., Fu, Y., Peng, S., Lian, X., et al., 2018. Extension of the growing season increases vegetation exposure to frost. Nat. Commun. 9, 426.
Ma, Q.Q., Huang, J.G., Hanninen, H., Berninger, F., 2019. Divergent trends in the risk of spring frost damage to trees in Europe with recent warming. Glob. Change Biol. 25, 351–360.
Mann, H.B., 1945. Nonparametric tests against trend. Econometrica 13, 245–259.
Meier, U., 1997. Growth stages of mono-and dicotyledonous plants. BBCH Monogr. Blackwell Wiss.-Verl. Berl. Wien.
Meng, L., Zhou, Y., Gu, L., Richardson, A.D., Penuelas, J., Fu, Y., et al., 2021. Photoperiod decelerates the advance of spring phenology of six deciduous tree species under climate warming. Glob. Change Biol. 27, 2914–2927.
Menzel, A., Helm, R., Zang, C., 2015. Patterns of late spring frost leaf damage and recovery in a European beech (*Fagus sylvatica* L.) stand in south-eastern Germany based on repeated digital photographs. Front. Plant Sci. 6.
Morin, X., Chuine, I., 2014. Will tree species experience increased frost damage due to climate change because of changes in leaf phenology? Can. J. For. Res. 44, 1555–1565.
Nolè, A., Rita, A., Ferrara, A.M.S., Borghetti, M., 2018. Effects of a large-scale late spring frost on a beech (*Fagus sylvatica* L.) dominated Mediterranean mountain forest derived from the spatio-temporal variations of NDVI. Ann. For. Sci. 75, 83.
R Core Team. (2023). R: A language and environment for statistical computing. *R Foundation for Statistical Computing*, Vienna, Austria.
Rigby, J.R., Porporato, A., 2008. Spring frost risk in a changing climate. Geophys. Res. Lett. 35.
Rubio-Cuadrado, A., Gomez, C., Rodriguez-Calcerrada, J., Perea, R., Gordaliza, G.G., Camarero, J.J., et al., 2021. Differential response of oak and beech to late frost damage: an integrated analysis from organ to forest. Agric. For. Meteorol., p. 297
Sangüesa-Barreda, G., Di Filippo, A., Piovesan, G., Rozas, V., Di Fiore, L., García-Hidalgo, M., et al., 2021. Warmer springs have increased the frequency and extension of late-frost defoliations in southern European beech forests. Sci. Total Environ. 775, 145860.
Scheifinger, H., Menzel, A., Koch, E., Peter, C., 2003. Trends of spring time frost events and phenological dates in Central Europe. Theor. Appl. Climatol. 74, 41–51.
Taschler, D., Beikircher, B., Neuner, G., 2004. Frost resistance and ice nucleation in leaves of five woody timberline species measured in situ during shoot expansion. Tree Physiol. 24, 331–337.
Vidal, J.P., Martin, E., Franchisteguy, L., Baillon, M., Soubeyroux, J.M., 2010. A 50-year high-resolution atmospheric reanalysis over France with the Safran system. Int. J. Climatol. 30, 1627–1644.
Vitasse, Y., Bottero, A., Cailleret, M., Bigler, C., Fonti, P., Gessler, A., et al., 2019. Contrasting resistance and resilience to extreme drought and late spring frost in five major European tree species. Glob. Change Biol. 25, 3781–3792.
Vitasse, Y., Lenz, A., Korner, C., 2014. The interaction between freezing tolerance and phenology in temperate deciduous trees. Front. Plant Sci. 5.
Vitasse, Y., Schneider, L., Rixen, C., Christen, D., Rebetez, M., 2018. Increase in the risk of exposure of forest and fruit trees to spring frosts at higher elevations in Switzerland over the last four decades, 248. Agric. For. Meteorol., pp. 60–69
Zohner, C.M., Mo, L.D., Renner, S.S., Svenning, J.C., Vitasse, Y., Benito, B.M., et al., 2020. Late-spring frost risk between 1959 and 2017 decreased in North America but increased in Europe and Asia. Proc. Natl. Acad. Sci. U.S.A. 117, 12192–12200.
Zohner, C.M., Rockinger, A., Renner, S.S., 2019. Increased autumn productivity permits temperate trees to compensate for spring frost damage. New Phytol. 221, 789–795.